Which Optical Smoothing for LMJ and NIF ?

J. Garnier

Centre de Mathématiques Appliquées, CNRS URA 756,
Ecole Polytechnique, 91128 Palaiseau Cedex, France.

C. Gouédard, L.Videau

Commissariat à l'Energie Atomique, Centre de Limeil-Valenton, 94195 Villeneuve Saint Georges.

A. Migus

Laboratoire pour l'Utilisation des Lasers Intenses, CNRS UMR 100,
Ecole Polytechnique, 91128 Palaiseau Cedex.

ABSTRACT

This paper is concerned with the statistical comparison of two-dimensional smoothing by spectral dispersion and smoothing by optical fiber, both techniques being proposed for uniform irradiation in plasma physics. In the asymptotic framework of a large number of elements of the random phase plate or excited optical modes of the fiber, closed-form expressions for the contrast and spatial spectrum of the integrated intensity of the speckle pattern are derived so as to put into evidence performance differences between these methods. These differences essentially originate from the much longer time delay induced by the multimode fiber with respect to the one induced by the gratings and from the interplay between the nature of the delay line vs. the nature of the spectral broadening.

Keywords: optical smoothing, statistical optics

1. INTRODUCTION

The implementation of smoothing techniques for uniform irradiation in plasma physics[1] has become an extensively studied object, specially in the light of the US National Ignition Facility project[2] and the French Laser MegaJoule project[3] for Inertial Confinement Fusion. All active smoothing methods: Induced Spatial Incoherence with echelons,[4] Smoothing by Spectral Dispersion (SSD) and random phase plate,[5] Smoothing by multimode Optical Fiber (SOF),[6] involve the illumination on the target with an intensity which is a time varying speckle pattern, so that the time integrated intensity averages towards a flat profile. The corresponding time varying speckle pattern relies on the same general concept. First a broadband pulse is generated either by a naturally incoherent broad source or a frequency modulated laser beam using phase modulators. In a next step this broadband source is spatially dispersed and spatial random modulations are imposed on the spectral components so as to produce on target a moving speckle pattern (with Gaussian statistics for the electric field).

However, if the principles are shared in common, it should be emphasized that the values of the characteristic parameters of each method may differ by as much as one or two orders of magnitude. This is particularly true for the time delay induced by the dispersion of the frequencies across the beam, which is created by the gratings in

SPIE Vol. 3047 • 0277-786X/97/$10.00

the SSD implementation or by a multimode fiber in the SOF implementation. This should imply quite different smoothing properties. For instance the distribution of the smoothed spatial frequencies will strongly depend on the selected method. We will focus our attention on two-dimensional SSD and SOF implementations and compare their respective properties. Our main aim is to derive closed-form expressions of the contrasts and power spectral densities of the smoothed fluence distributions, in order to get general laws for statistical properties of smoothing techniques. In Section 2 we review the elementary concepts behind smoothing techniques while the next two sections are devoted to SSD and SOF. Section 5 discusses some advanced concepts about the smoothed focal spots.

2. A SIMPLIFIED INTRODUCTION TO OPTICAL SMOOTHING

2.1. Basic principles

The principle of optical smoothing consists of generating a time varying speckle pattern, whose coherence time is as short as possible. This implies that broadband long pulses are needed. The time integrated intensity is then a sum of N independent patterns, where N is the ratio of the integration time over the coherence time of the light. As a consequence the fluctuations of the integrated intensity average towards 0 (strong law of large numbers[8]). More exactly the contrast (i.e. the ratio of the variance over the mean intensity) will be reduced by $\sqrt{N}$.

The ideal principle of SSD is the following.[5,9,2] A broadband source is spectrally dispersed onto a random phase plate (RPP), which consists of square elements imposing randomly a phase shift of 0 or π. Each square element of the RPP is illuminated by a different frequency. The beamlets generated by the elements focus onto the target; they interfere and form a speckle pattern. The key point is that the phases of the beamlets will vary in time according to their respective illumination frequencies. As a result the interference terms between the different beamlets will average to zero, so that the integrated intensity will approach the smooth sinc^2 envelope. However, if several of the elements of the RPP are illuminated by the same frequency, there will be residual correlations and unsmoothed structure will exist in the integrated intensity. This will be actually the case in any realistic configuration.

In this section we focus our attention on one-dimensional SSD (1D SSD), whose standard implementation is shown in Fig. 1. An incident monochromatic beam with wavelength λ_0 is spectrally broadened by a sinusoidal phase modulator with frequency ν and depth β. The spectrum consisting of about 2β sidebands is dispersed onto the RPP by a grating which induces a lateral time delay T_d.

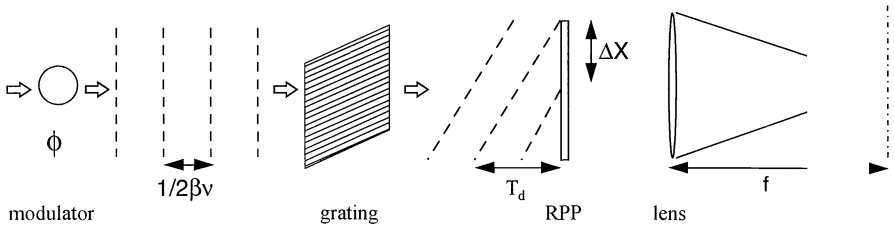

Fig. 1. Standard implementation of 1D SSD.

Let us look at how separated points in the near field interfer and contribute to the generation of the speckle pattern. In the plane of the RPP the incident beam splits into elementary beams with diameter $\Delta X \sim D/(2\beta\nu T_d)$ where D is the near field beam aperture. Points of the RPP which are separated by less than ΔX are illuminated by the same frequency. Two successive sideband beams are uncorrelated, but two sideband beams separated by

$D/(\nu T_d)$ are coherent, since the modulation is sinusoidal. As a consequence about 2β uncorrelated sidebands can be created. So we can expect an asymptotic contrast reduction equal to $\sqrt{2\beta}$.

Two elements of the RPP separated by less than ΔX are coherently illuminated. The angle of the interference between two points separated by ΔX is given by $\Delta\theta = \Delta X/f$, where f is the lens focal length. Thus these points contribute to spatial frequency on the target given by $\nu_x = \Delta\theta/\lambda_0 = \Delta X/(f\lambda_0)$. So the spatial frequencies on the target (in the dispersion direction) less than $\Delta X/(f\lambda_0) = D/(2\lambda_0 f\beta\nu T_d)$ are not smoothed. Neither are the spatial frequencies multiple of $D/(\lambda_0 f\nu T_d)$, owing to the pure sinusoidal phase modulation. In what follows we shall exhibit analytical expressions which will appear consistent with the heuristical arguments developed here above.

2.2. Statistical analysis

We aim at showing that statistical theory may be used to perform an efficient study of the smoothing performances of the different methods. From a practical point of view the fluence distribution over some surface Σ is examined: $(I(t,x))_{x\in\Sigma}$. We introduce the spatial measure, denoted by μ, which connects to any functional $f(I)$ the spatial average $|\Sigma|^{-1}\int_\Sigma f(I)(x)dx$. So we are looking for data about the measure μ, which depends on the realization of the pattern that is observed.

From a theoretical point of view, we are going to carry out statistical averages with respect to the possible realizations of the patterns, which correspond to the possible realizations of the experimental devices. The randomness holds in the fluctuations of the radius or the index of refraction of the fiber core in the SOF case, and in the random phases imposed by the elements of the RPP in the SSD case. This average is denoted by $< . >$ and carried out in some fixed point x in Σ.

If the field is spatially ergodic, then the spatial measure μ and the statistical measure $< . >$ coincide for a well-chosen surface Σ, where the field is macroscopically similar, but microscopically moving. *It is equivalent to compute a statistical average over all possible realizations in some fixed point x and to compute a spatial average over $x \in \Sigma$ for some given realization.* That will be actually the case in the configurations that will be examined throughout the paper.

2.3. Generation of long broadband pulses

The spectral broadening is obtained by imposing a phase modulation to the monochromatic incident beam. Such a method is of great interest for the technique of SSD. Indeed in (and near) the relay image planes of the gratings the pure phase modulation does not induce any amplitude modulation. As a consequence, if the amplifiers lie in these planes, the amplification performance is equivalent to that of a spatially smooth clean beam. On the other hand, in the SOF configuration, unavoidable large spatial fluctuations in intensity induce large nonlinear effects which have been observed to reduce the amplification efficiency.[7]

In order to make the comparison meaningful, we shall compare the smoothing performances of SSD and SOF techniques with the same spectral broadenings. So we shall assume in the following that similar phase modulators are used in the SSD and SOF configurations, although natural broadband sources are generally used in the latter case. We shall consider in this paper two different phase modulation methods. We shall use on the one hand pure sinusoidal phase modulator

$$\phi_{spm}(t) = \beta\sin(2\pi\nu t), \tag{1}$$

with depth β and frequency ν, and on the other hand random phase modulator

$$\phi_{rpm}(t) = \sigma f(t/t_c), \tag{2}$$

where σ is the amplitude of the modulation and t_c is the correlation time. The production of modulations with random properties will be discussed in the last section. We shall assume that f obeys stationary Gaussian statistics, with mean 0 and Gaussian correlation function:

$$\mathbb{E}[f(t)] = 0, \quad \mathbb{E}[f(t)f(t')] = e^{-(t-t')^2}, \tag{3}$$

where $\mathbb{E}$ stands for statistical averaging with respect to the distribution of the process f. Such a process is time ergodic, so that the time average $< . >_t$ coincides with $\mathbb{E}$. In what follows we shall compare the performances of sinusoidal and random modulators. So it is convenient to establish the relations between the scalars which characterize them. An efficient way consists of analyzing the autocorrelation functions:

$$< \phi_{spm}(t)\phi_{spm}(t+\Delta t) >_t = \frac{\beta^2}{2}\cos(2\pi\nu\Delta t) \simeq \frac{\beta^2}{2}\left(1 - 2\pi^2\nu^2\Delta t^2\right), \text{ if } \Delta t \ll \nu^{-1}, \tag{4}$$

$$\mathbb{E}\left[\phi_{rpm}(t)\phi_{rpm}(t+\Delta t)\right] = \sigma^2 \exp\left(-\frac{\Delta t^2}{t_c^2}\right) \simeq \sigma^2\left(1 - \frac{\Delta t^2}{t_c^2}\right), \text{ if } \Delta t \ll t_c. \tag{5}$$

Therefore, in the comparisons it will be consistent to identify $\beta = \sqrt{2}\sigma$ and $\sqrt{2}\pi\nu = t_c^{-1}$. Taking into account these relations, a sinusoidal modulator and a random modulator involve spectral broadenings whose full bandwidth extents are similar. However it should be emphasized that a sinusoidal phase modulator with frequency ν and depth β produces a *discrete* spectrum consisting of about 2β lines separated by $2\pi\nu$ (see Fig. 2), while a random phase modulator produces a *continuous* spectrum of full bandwidth extent $\sim 4\sigma/t_c$.

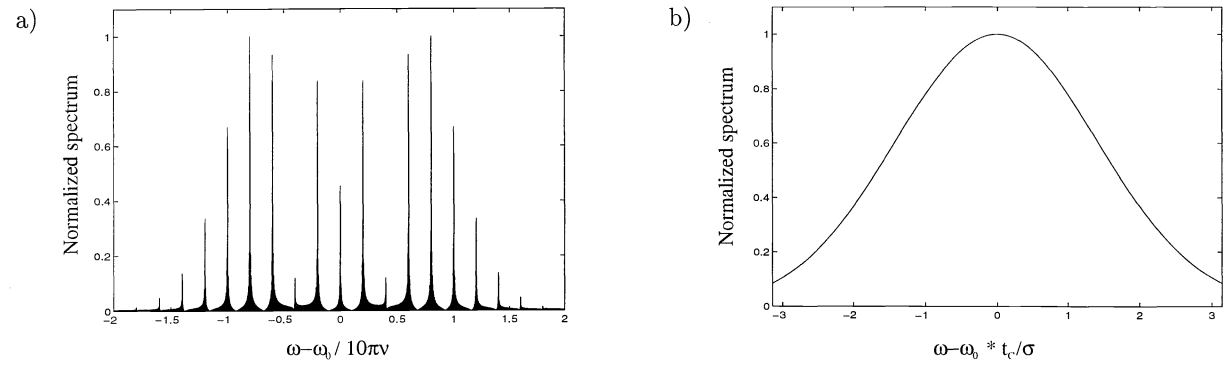

Fig. 2a. Spectral broadening imposed by a sinusoidal phase modulator with depth $\beta = 5$.
Fig. 2b. Spectral broadening imposed by a random phase modulator with amplitude $\sigma = 5/\sqrt{2}$.

The spectral filling uniformity will appear essential for the smoothing efficiency. Regardless of the method, the coherence time of a beam with full bandwidth $\Delta\nu$ is larger than $1/\Delta\nu$. Thus the maximal reduction of the contrast for time integration T is $\sqrt{\Delta\nu T}$. It appears that the larger the bandwidth, the more rapidly the contrast will be reduced.[9] However the full bandwidth extent is not the single determinant parameter. Another important parameter is the number N_{max} of uncorrelated speckle patterns which can be generated by a beam with bandwidth $\Delta\nu$. If the spectrum is continuous, then N_{max} is given by the ratio $\Delta\nu/\delta\nu_{ind}$, where $\delta\nu_{ind}$ is the minimum frequency shift required to decorrelate the speckle patterns generated by two monochromatic beams of different frequencies. $\delta\nu_{ind}$ depends only on the dispersive properties of the selected smoothing method and is conversely proportional to the induced time delay. If the spectrum is discrete, N_{max} may be inferior to the ratio $\Delta\nu/\delta\nu_{ind}$, because the holes in the spectrum cannot obviously generate a speckle. So a more adequate and general definition of N_{max} is the number of spectral bands of bandwidth $\delta\nu_{ind}$ that can be inserted in the effective spectrum.

As an example we can consider the spectral broadening generated by a sinusoidal phase modulator. We deal with about 2β monochromatic lines whose frequencies are separated by ν. If $\nu > \delta\nu_{ind}$, then the speckle patterns generated by the lines of the spectrum are uncorrelated. We can set one band with bandwidth $\delta\nu_{ind}$ on every line, so N_{max} is equal to 2β and the asymptotic contrast reduction will be equal to about $\sqrt{2\beta}$. If $\nu < \delta\nu_{ind}$, then the speckle patterns generated by the lines of the spectrum are correlated. The discrete spectrum is actually equivalent to a continuous spectrum because the dispersive component does not resolve the lines. Then N_{max} is given by the ratio $2\beta\nu/\delta\nu_{ind}$, which is inferior to 2β.

3. SMOOTHING BY SPECTRAL DISPERSION (SSD)

3.1. Implementation

It appears that smoothing by 1D SSD is insufficient to reach the required level of uniformity for direct drive inertial confinement fusion. On the one hand we cannot expect to obtain the required contrast reduction of 1 per cent,[1] and on the other hand only the spatial frequencies in the dispersion direction are smoothed. The performance of SSD can be greatly improved if the beam is dispersed in both orthogonal directions. A straightforward implementation of 2D SSD is shown in Fig. 3.[9] The spectral dispersion is obtained by applying a phase modulator then a grating in each orthogonal direction. An auxiliary grating is imposed before each modulator in order to compensate for the temporal skew of the global shape of the field. The input beam is a monochromatic pulse with pulsation ω_0 and duration T_{pulse} (of the order of several nanoseconds). We denote by T_{dj} the time delays induced by the gratings and by r_c the correlation radius of the speckle pattern:

$$T_{dj} = s_j D, \quad r_c = \frac{\lambda_0 f}{D}, \tag{6}$$

where s_j is the temporal skew per unit length generated by the grating in the x-direction for $j = 1$ and in the y-direction for $j = 2$. We shall compute the characteristics of the smoothed pattern in the asymptotic framework of a very large number of elements of the RPP.

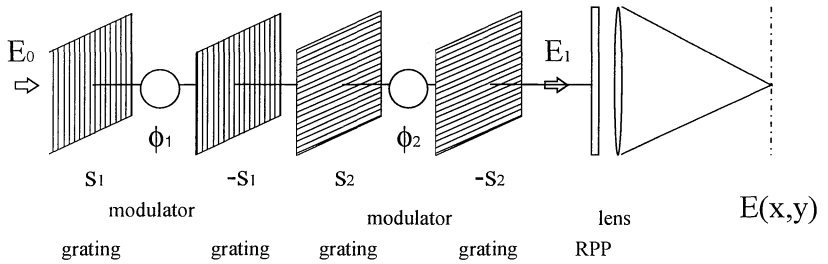

Fig. 3. Standard implementation of 2D SSD.

3.2. Sinusoidal modulations

We consider pure sinusoidal phase modulators. β_j and ν_j are respectively the modulation depths and frequencies of the modulators in the x-direction for $j = 1$ and in the y-direction for $j = 2$. The field which illuminates the RPP has the following form:

$$E_1(t,x,y) = E_0(t) \exp i \left(\beta_1 \sin(2\pi\nu_1(t + s_1 x)) + \beta_2 \sin(2\pi\nu_2(t + s_2 y))\right). \tag{7}$$

We shall assume that the time delays are longer than the modulation periods, which writes $\nu_j T_{dj} \geq 1$. The condition $\nu T_d \geq 1$ means that the modulator effectively modulates over the time delay induced by the gratings.

As a consequence the dispersor (consisting of the gratings) resolves the lines of the spectrum of the modulated beam. The speckle patterns generated by the lines of the spectrum are uncorrelated, which produces an optimal contrast reduction. The smoothed contrast $c(T)$ for integration time T is given by[10]:

$$c(T)^2 = \sum_{m,n=-\infty}^{+\infty} \operatorname{sinc}\left((m\nu_1 + n\nu_2)T\right)^2 a_m(\beta_1)a_n(\beta_2), \tag{8}$$

where the positive coefficients $a_n(\beta)$ depend only on the modulation depth β and can be expressed by means of the Bessel functions:

$$a_n(\beta) = \sum_{m=-\infty}^{+\infty} J_{m+n}(\beta)^2 J_m(\beta)^2. \tag{9}$$

If the modulation frequencies ν_1 and ν_2 are incommensurate, then for long integration times the contrast tends to its minimal value:

$$c^2 = a_0(\beta_1)a_0(\beta_2). \tag{10}$$

More exactly, if $|m\nu_1/\nu_2 - n| < \eta/\beta$, then the field which illuminates the RPP satisfies $E_1(t + n/\nu_1, x, y) \simeq E_1(t, x, y)$ if η is small enough ($\eta < 1/(2\pi)$). So the pattern in the focal plane of the lens repeats itself after $\Delta t = n/\nu_1$, exactly if $\eta = 0$ and approximatively if η is small enough. If n and m are larger than β, then there is no effect of the commensuracy relation between the modulation frequencies, because the contrast has enough time to reach the asymptotic value (10). But if n or m is smaller, then the effect on the contrast reduction is noticeable. This can be derived also from the study of expression (8). Indeed the support of $n \mapsto a_n(\beta)$ lies roughly in $[-\beta, \beta]$ for large β, which puts into evidence that a commensuracy relation between ν_1 and ν_2 with integers n, m larger then β does not affect the smoothing performance. Throughout the paper, we will say that the frequencies ν_1 and ν_2 are commensurate if there exists integers n, $m \in [-\beta, \beta]$ such that

$$\left| m\frac{\nu_1}{\nu_2} - n \right| < \frac{1}{2\pi\beta}. \tag{11}$$

When the frequency modulations are incommensurate, the contrast (8) decreases as $\sqrt{T}$ for small integration times T. More exactly, if ν_1 and ν_2 are close to the same value ν and incommensurate, then the contrast decreases as $\sqrt{\nu T / \sum a_n^2(\beta)} \sim \sqrt{4\beta\nu T}$ for small integration time T, until it reaches the asymptotic value (10) for integration times of the order of β/ν. Fig. 4 represents the evolution of the smoothed contrast as a function of the integration time T for different modulation frequencies. In particular, comparing the case $\nu 1 = 1$ Ghz, $\nu 2 = 1.05$ Ghz with the case $\nu 1 = 1$ Ghz, $\nu 2 = 1.1$ Ghz, it appears that the contrast reduction in the second one is more rapid, because the ratio of the modulation frequencies in the first configuration nearly satisfies (11) with $n = m = 1$. On the contrary, when the frequencies are commensurate (case $\nu 1 = 1$ Ghz, $\nu 2 = 1$ Ghz or else $\nu_1 = 1$ Ghz, $\nu_2 = 2$ Ghz in Fig. 4), then the smoothed contrast never reaches the optimal value (10), but stops at some higher value.

Let us examine the asymptotic smoothed fluence distribution when the modulation frequencies ν_1 and ν_2 are incommensurate. The smoothed power spectral density $\mathcal{G}_s(\nu_x, \nu_y)$ is equal to[10]:

$$\mathcal{G}_s(\nu_x, \nu_y) = \delta(\nu_x, \nu_y) + r_c^2 \mathcal{G}_{s1}(r_c\nu_x)\mathcal{G}_{s2}(r_c\nu_y), \text{ with } \mathcal{G}_{sj}(\alpha) = \Lambda(\alpha) J_0^2\left(\sqrt{2}\beta_j\sqrt{1 - \cos(2\pi\nu_j T_{dj}\alpha)}\right), \tag{12}$$

where $\Lambda(\alpha) = 1 - |\alpha|$ if $|\alpha| \leq 1$, and $\Lambda(\alpha) = 0$ if $|\alpha| > 1$. The power spectral densities (PSD) are plotted in Fig. 5 (we do not represent the Dirac function, which is due to the non-zero mean intensity of the speckle pattern).

The spatial frequencies below $h_0/(2\pi\beta\nu_j T_{dj} r_c)$, ($j = 1$ in the x-direction and $j = 2$ in the y-direction) are not smoothed ($h_0 \simeq 1.1$ is such that $J_0(h_0) = 1/\sqrt{2}$). Moreover the spectrum appears concentrated near some particular spatial frequencies, which are multiple of $\Delta\nu_x = 1/(\nu_1 T_{d1} r_c)$ in the x-direction and of $\Delta\nu_y = 1/(\nu_2 T_{d2} r_c)$ in the y-direction. This is due to the use of pure sinusoidal modulation and a more advanced phase modulation will break this resonant structure. These results are consistent with the heuristical arguments of Section 2.

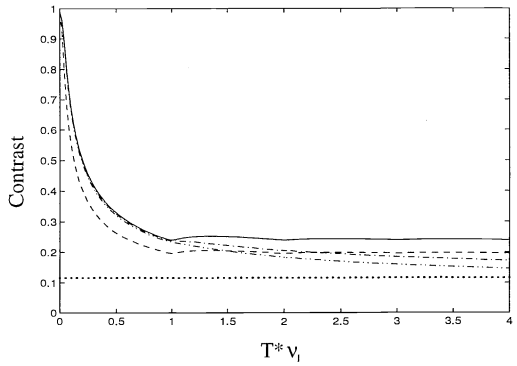

Fig. 4. Variation of the contrast with integration time - 2D SSD with different sinusoidal modulations, with $\beta_j = 5$ and $\nu_j T_{dj} \geq 1$ for $j = 1, 2$. The dotted line represents the asymptotic optimal contrast (10). In solid (resp. dashed, dot-dashed, dot-dot-dashed) line is plotted the case $\{\nu_1 = 1$ Ghz, $\nu_2 = 1$ Ghz$\}$ (resp. $\{\nu_1 = 1$ Ghz, $\nu_2 = 2$ Ghz$\}$, $\{\nu_1 = 1$ Ghz, $\nu_2 = 1.05$ Ghz$\}$, $\{\nu_1 = 1$ Ghz, $\nu_2 = 1.1$ Ghz$\}$).

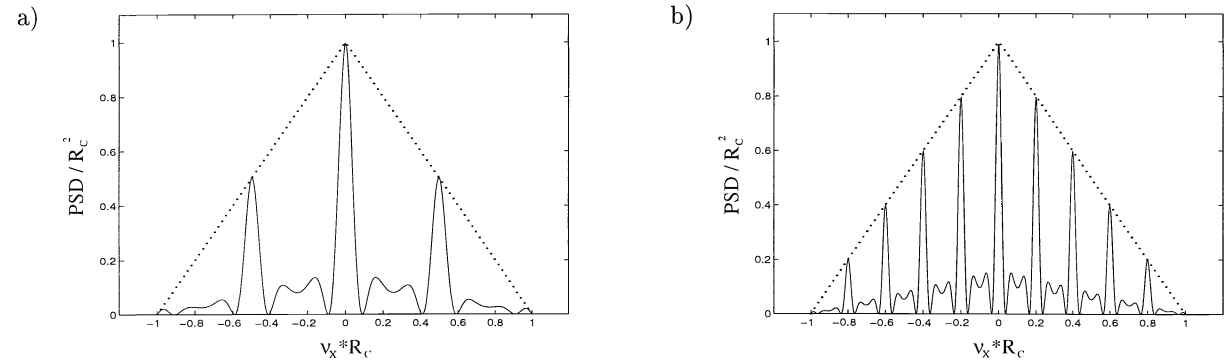

Fig. 5a. Normalized power spectral densities in the x-direction - 2D SSD for different sinusoidal modulations. The dotted (resp. solid) lines represent the densities of the unsmoothed (resp. smoothed) speckle pattern. The modulation depth is taken to be equal to 5 and $T_{d1}\nu_1 = 2$.
Fig. 5b. Idem with $T_{d1}\nu_1 = 5$.

3.3. Random modulations

We aim now at studying the 2D SSD implementation of Fig. 3 when using two independent random phase modulators (2) with the same amplitudes σ and correlation times t_c. In order to simplify the notations we shall assume moreover that the time skews per unit length generated by the gratings are both equal to s, so that each grating introduces the same time delay $T_d = sD$. We also assume that $\sigma T_d > t_c$, which means that the full bandwidth extent $\sim \sigma/t_c$ is larger than the frequency shift necessary to decorrelate the speckle pattern. The power spectral density of the smoothed speckle pattern for integration time $T > t_c/\sigma$ can then be expressed in a complicated closed-form expression:

$$\mathcal{G}_T(\nu_x, \nu_y) = \delta(\nu_x, \nu_y) + r_c^2 \Lambda(r_c\nu_x)\Lambda(r_c\nu_y)\frac{2}{T^2}\int_0^T dt(T-t)\psi(\frac{T_d}{t_c}r_c\nu_x, \frac{t}{t_c})\psi(\frac{T_d}{t_c}r_c\nu_y, \frac{t}{t_c}), \tag{13}$$

where $\psi(\alpha_1, \alpha_2) = \exp\left(-\sigma^2\left(2 - 2e^{-\alpha_1^2} - 2e^{-\alpha_2^2} + e^{-(\alpha_1-\alpha_2)^2} + e^{-(\alpha_1+\alpha_2)^2}\right)\right)$, $\Lambda(\alpha) = 1 - |\alpha|$ if $|\alpha| < 1$ and $\Lambda(\alpha) = 0$ otherwise (see Fig. 6). Integrating the power spectral density over the spatial frequencies, we can deduce the contrast:

$$c^2 = \frac{\gamma_1^2 \pi t_c^2}{2\sigma^2 T_d^2} + \frac{\sqrt{\pi}\gamma_1 t_c}{\sigma T}, \tag{14}$$

where $\gamma_1 \simeq 1.25$. When the integration time belongs to the interval $[t_c/\sigma, t_c]$, it appears in Fig. 6 that the frequencies below $\sqrt{\ln 2}t_c^2/(\sqrt{2}T_d T r_c)$ are not yet smoothed. After this transition regime, i.e. for integration times $T > t_c$, the spatial frequencies above $\sqrt{\ln 2}t_c/(\sqrt{2}\sigma T_d r_c)$ are smoothed according to the expected rate $\sqrt{T}$. However the frequencies below $\sqrt{\ln 2}t_c/(\sqrt{2}\sigma T_d r_c)$ are very poorly smoothed.

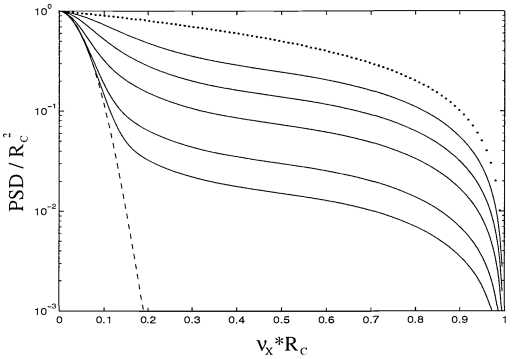

Fig. 6. Normalized power spectral densities - 2D SSD with random modulations. The dotted line represents the density of the unsmoothed pattern. The densities of the smoothed patterns integrated over $T = 0.5t_c$, $T = t_c$, $T = 2t_c$, $T = 5t_c$ and $T = 10t_c$ are successively plotted in solid lines. The dashed line represents the asymptotic power spectral density which corresponds to an infinite pulse time and an infinite integration time. The modulation amplitude is taken to be equal to $\sigma = 5/\sqrt{2}$ and the time delay $T_d = 3t_c$.

4. SMOOTHING BY OPTICAL FIBER (SOF)

4.1. Implementation

A broadband source illuminates a long multimode fiber. Although a natural broadband source is generally used in this configuration, for better comparison we consider a monochromatic source spectrally broadened by a phase modulator. The implementation is represented in Fig. 7. The incident beam excites many optical modes, which propagate according to different velocities. Moreover small random fluctuations of the core radius or of the index of refraction affect the propagation by introducing random phases into the modes. If the fiber is long enough, these phases can be considered as independent processes which obey uniform distributions over $[0, 2\pi]$.[12] As a consequence the optical modes interfer at the output of the fiber and their superposition produces a speckle pattern. If the propagation in the amplifier chain is linear, then the properties of the speckle pattern on the target are the same as the ones at the output of the fiber. We denote by T_d and r_c the time delay induced by the fiber and the correlation radius of the pattern at the end of the fiber (n is the index of the core):

$$T_d = \frac{L\theta^2}{8nc}, \quad r_c = \frac{\lambda_0}{\theta}. \tag{15}$$

We shall give the results in the asymptotic framework of an infinite number of optical modes. We shall assume also that the time delay induced by the fiber, which can be made as long as desired, is of the order of the pulse duration.

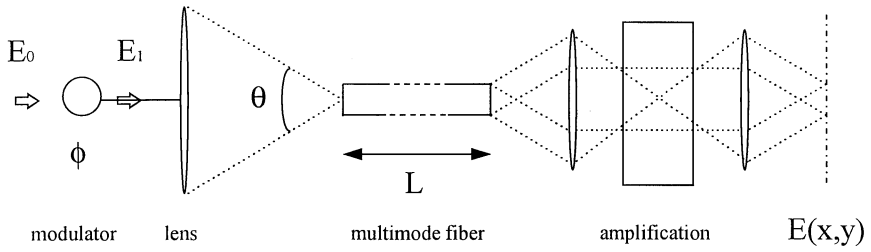

Fig. 7. Standard implementation of SOF.

4.2. Sinusoidal modulations

In order to compare the respective smoothing performances of 2D SSD and SOF, we shall assume that the phase modulator ϕ consists of the same modulators as those considered for 2D SSD. So we first assume in this section that $\phi(t) = \beta_1 \sin(2\pi\nu_1 t) + \beta_2 \sin(2\pi\nu_2 t)$, where β_j is the depth and ν_j the frequency of the jth modulator. If the frequencies ν_1 and ν_2 are incommensurate, then the power spectral density of the smoothed pattern for integration time T is equal to[10]:

$$\mathcal{G}_T(\nu_x, \nu_y) = \delta(\nu_x, \nu_y) + c^2(T) r_c^2 G(r_c \sqrt{\nu_x^2 + \nu_y^2}), \tag{16}$$

where the contrast $c(T)$ is given by (8), $G(x) = 8/\pi^2 \left(\arccos(x) - x\sqrt{1-x^2}\right)$ if $x \in [0,1]$ and $G(x) = 0$ otherwise (see Fig. 8). So it appears that the contrasts of the patterns smoothed by 2D SSD and by SOF are similar. However the spatial spectra are very different. While the smoothing rate depends strongly on the spatial frequency for SSD, the striking point is that SOF smoothes all spatial frequencies equally.

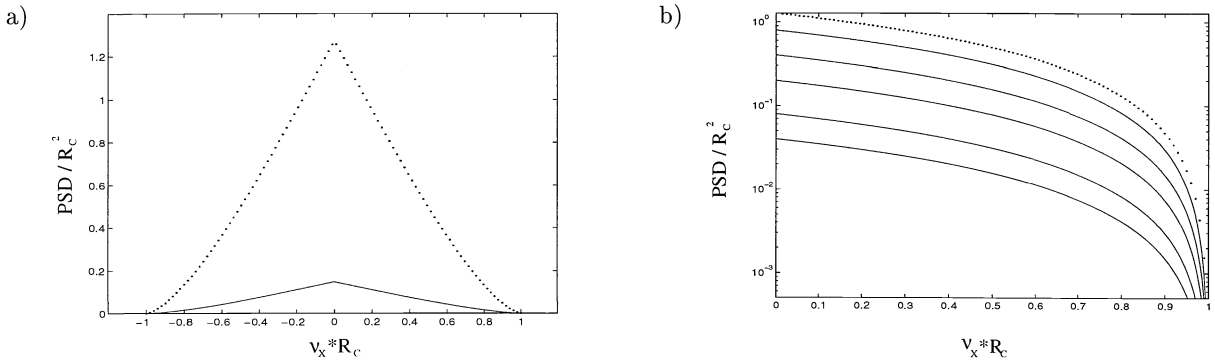

Fig. 8a. Normalized power spectral densities - SOF with two sinusoidal modulators with depth 5 and incommensurate frequencies. The dotted (resp. solid) line represents the density of the unsmoothed (resp. smoothed) pattern.
Fig. 8b. Normalized power spectral densities - SOF with two independent random modulators. The densities of the unsmoothed pattern (dotted line) and of the smoothed patterns (solid lines) are represented for successive integration times $T = 0.5t_c$, $T = t_c$, $T = 2t_c$, $T = 5t_c$ and $T = 10t_c$. The modulation amplitude is taken to be equal to $\sigma = 5/\sqrt{2}$.

As a remark, notice that the results which have been presented here above hold true in the approximation $\nu_j T_d \gg 1$, which is obviously fulfilled with standard integrated optic phase modulators because of the long time delay induced by the fiber. If we take into account the finite parameter νT_d, then the results are modified according to the following way. The power spectral density is given by (16) for spatial frequencies above $1/(2\beta\nu T_d r_c)$. Spatial frequencies below this one are not smoothed actually. However if we adopt phase modulators with frequencies

10 Ghz and depth 5 combined with a 100 m long fiber, which generates a 5 ns time delay, then only the spatial frequencies below $1/(500r_c)$ are not smoothed. This frequency band is far from the frequencies which can be resolved, since they correspond to spatial sizes of several millimeters, which are larger than the fiber output or the focal spot. So we can consider than the previous results hold true for the relevant frequencies.

4.3. Random modulations

We now assume that the phase modulator ϕ consists of two independent random phase modulators (2) with the same amplitudes σ and correlation times t_c. We find that the contrast of the smoothed pattern for integration time T is equal to:

$$c(T)^2 = \frac{\gamma_1 \sqrt{\pi} t_c}{\sigma T}, \tag{17}$$

where $\gamma_1 \simeq 1.25$. So the contrast decreases according to the expected $\sqrt{T}$ rate. Indeed N uncorrelated speckle patterns are generated during a time interval of duration T, where $N \sim \sigma T/t_c$, and the contrast decreases as $\sqrt{N}$. It is interesting to notice that the contrast reductions obtained by either random or sinusoidal modulations are similar for small integration times, as shown by Fig. 9. But for integration times longer than t_c the contrast obtained with sinusoidal modulations reaches its asymptotic value (10), while the contrast obtained with random modulations goes on decreasing according to the rate $\sqrt{T}$.

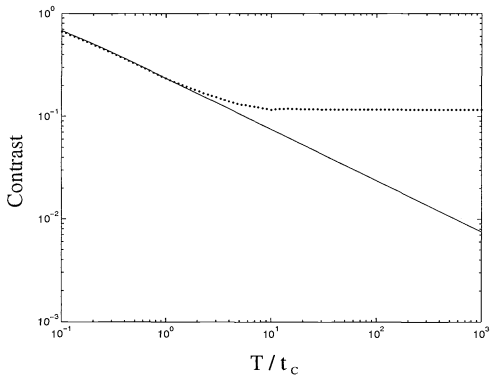

Fig. 9. Variation of the contrast with time integration - SOF. The solid line corresponds to a phase modulation generated by two independent random modulators with the same amplitude $\sigma = 5/\sqrt{2}$ and correlation time t_c. In dotted line is plotted the contrast reduction when using two sinusoidal phase modulators with depth $\beta = 5$ and frequencies $\nu_1 = 0.9/(\sqrt{2}\pi t_c)$, $\nu_2 = 1.1/(\sqrt{2}\pi t_c)$ respectively.

The power spectral density of the time integrated intensity is given by (16) combined with the expression of contrast (17) and is plotted in Fig. 8.

5. SMOOTHED FOCAL SPOTS

There exists another advantage of the SOF technique, which does not appear in the statistical properties of the smoothing. It concerns the envelope of the fluence distribution. Let us first examine the instantaneous focal spots. In the SSD case the envelope is the diffraction function of an element of the phase plate, which is a sinc^2 in the case of the RPP. As a consequence some energy is lost in the tail of this envelope. Such a drawback can be compensated by using a Kinoform Phase Plate (KPP). Instead of steeply passing from 0 to π in the case of a RPP, the random phases of the elements of a KPP continuously go from 0 to π, so that the diffraction function

can become as flat as a 12th power super-Gaussian.[13] However this technique is somewhat complicated and expensive. In the case of the SOF technique, the fiber output is imaged onto the target. Thus the whole energy in the target plane is contained uniformly in the fiber output image, which is a convenient way to realize a very high order super-Gaussian irradiance profile.

Let us now examine the time evolution of the focal spots and the envelop of the smoothed focal spots. The focal spot generated by the RPP depends on the spectrum and the dispersion and moves in all directions. It presents two serious drawbacks. First the smoothed focal spot has a larger size than the instantaneous spot, and is not a super-Gaussian anymore, even if you use a KPP. Second all speckle patterns do not overlap, so the expected contrast reduction is not reached, especially near the boundaries of the smoothed focal spot. On the other hand, the focal spot generated by the SOF technique does not depend on the spectrum nor the dispersion. So the smoothed focal spot has the same profile as the instantaneous one.

6. CONCLUSION

The comparison of the SOF and 2D SSD techniques puts into evidence that SOF presents two advantages:
1) The cut-off frequency (below which the spatial frequencies are not smoothed) is conversely proportional to the time delay. Thus 2D SSD does not smooth a somewhat large band of low spatial frequencies, while SOF is able to smooth all relevant frequencies equally.
2) The focal spot generated by the SOF technique has a better behavior with respect to the side-effects of the smoothing than the one generated by SSD.

While the smoothing performance of SOF is greater than that of 2D SDD, the amplification performance is strongly affected by the fact that the beam has large intensity fluctuations. The great advantage of 2D SSD is that the beam is only phase modulated, which does not affect amplification. On the opposite an anomalous intensity saturation has been observed in the amplification of intense pulses which had been smoothed by SOF in a large Nd-glass power chain.[7] It has appeared that the laser output energy was only one half of what one usually obtains with a clean near field. We are now developing a statistical nonlinear model in order to explain this intensity saturation. This theory is based on the fact that self-phase modulation due to strong temporal amplitude fluctuations creates new wavelengths scattered in the tail of the gain profile. However this theory should be extended to spatial effects and filamentation to fully explain the observed saturation effect.

7. ACKNOWLEDGEMENTS

We thank J. Paye and C. Sauteret for useful and stimulating discussions. This work was performed under the auspices of the Laser MegaJoule Program of CEA/DAM and the GDR POAN (Groupe De Recherches "Propagation des Ondes en milieux Aléatoires et / ou Non-linéaires") of CNRS.

8. REFERENCES

[1] R. H. Lehmberg and S. P. Obenschain, "Use of induced spatial incoherency for uniform illumination," *Optics Comm.* **46**, 27-31 (1983).

[2] J. E. Rothenberg, "SSD with generalized phase modulation," NIF-LLNL-96-02, December 27, 1995.

[3] LMJ Project: APS 94 proposition, CEA/DAM Palen program.

[4] R. H. Lehmberg, A. J. Schmitt, and S. E. Bodner, "Theory of induced spatial incoherence," *J. Appl. Phys.* **62**, 2680-2701 (1987).

[5] S. Skupsky, R. W. Short, T. Kessler, R. S. Craxton, S. Letzring, and J. M. Soures, "Improved laser-beam uniformity using the angular dispersion of frequency-modulated light," *J. Appl. Phys.* **66**, 3456-3462 (1989).

[6] D. Véron, H. Ayral, C. Gouédard, D. Husson, J. Lauriou, O. Martin, B. Meyer, M. Rostaing, and C. Sauteret, "Improved laser-beam uniformity using the angular dispersion of frequency-modulated light," *Optics Comm.* **65**, 42-45 (1988).

[7] D. Véron, G. Thiell, and C. Gouédard, "Optical smoothing of the high power Phebus Nd-glass laser using the multimode optical fiber technique," *Optics Comm.* **97**, 259-271 (1993).

[8] J. W. Goodman, "Statistical properties of laser speckle patterns," in *Laser speckle and related phenomena*, J. C. Dainty, ed. (Springer-Verlag, Berlin, 1984), pp. 9-75.

[9] J. E. Rothenberg, "Two-dimensional smoothing by spectral dispersion for direct drive inertial confinement fusion," in *Solid state lasers for applications to ICF*, M. André and H. T. Powell, eds. (Society of Photo-Optical Instrumentation Engineers, Vol. 2633, 1995), pp. 634-644.

[10] J. Garnier, C. Gouédard, and A. Migus, "A statistical comparison of Smoothing by Spectral Dispersion vs. multimode Optical Fiber," submitted.

[11] D. Middleton, *Introduction to statistical communication theory* (Mc Graw Hill, New York, 1960), p. 141.

[12] B. Moleshi, J. W. Goodman, and E. G. Rawson, "Bandwidth estimation for multimode optical fibers using the frequency correlation function of speckle patterns", *Appl. Opt.* **22**, 995-999 (1983).

[13] S. N. Dixit, M. C. Rushford, I. M. Thomas, and M. D. Perry, "Continuous contour phase plates for tailoring the focal plane irradiance profile", in *Solid state lasers for applications to ICF*, M. André and H. T. Powell, eds. (Society of Photo-Optical Instrumentation Engineers, vol. 2633, 1995), pp. 141-151.